Cellulose (2024) 31:10915–10929
https://doi.org/10.1007/s10570-024-06271-3

ORIGINAL RESEARCH

Detection of pesticides in sprayed droplets by using biowaste-derived nanocellulose-based SERS nanosubstrate

Lynn R. Terry · Jacob W. Kruel · Manan Jain · Alison Lara · Priyanka Sharma · Benjamin S. Hsiao · Huiyuan Guo

Received: 23 June 2024 / Accepted: 1 November 2024 / Published online: 10 November 2024

Abstract The increased demand for agricultural productivity to support the growing population has resulted in the expanded use of pesticides. However, modern pesticide applications contaminate air, water, soil, and unintentional target species. It is necessary to develop effective and sustainable methods to detect different pesticides within our environment. Surface-enhanced Raman spectroscopy (SERS) has garnered significant attention for its ability to detect and quantify environmental contaminants, as it is a rapid and sensitive technique that requires minimal sample preparation. The present study demonstrates the development of a biowaste-derived nanocellulose-based thin-film that, when integrated with gold nanoparticles, produces a sustainable and reproducible SERS nanosubstrate. In this study, three pesticides (carbaryl, ferbam, and thiabendazole) were sensitively and selectively detected by the combined use of this novel nanocellulose-based SERS nanosubstrate and a portable Raman instrument. The limits of detection were determined to be 1.34, 1.01, and 1.41 mg/L for carbaryl, ferbam, and thiabendazole, respectively, all of which are well below the agricultural application concentrations recommended. SERS signals were collected for both prepared ferbam spray solution and collected sprayed droplets, and it was found that there is no major difference in the signals, indicating that this detection method is reliable to detect pesticide droplets. A commercial pesticide was detectable by the biowaste-derived SERS nanosubstrate. This study is among the first to utilize biowaste-derived nanocellulose to create SERS nanosubstrate for pesticide detection in spray droplets. We demonstrate the high potential of biowaste-derived nanocellulose in combination with the portable Raman technique for agricultural pesticide spray detection.

Supplementary Information The online version contains supplementary material available at https://doi.org/10.1007/s10570-024-06271-3.

L. R. Terry · J. W. Kruel · M. Jain · A. Lara · H. Guo (✉)
Department of Chemistry, State University of New York at Binghamton, Binghamton, NY 13902, USA
e-mail: hguo@binghamton.edu

P. Sharma
Department of Chemical and Paper Engineering, Western Michigan University, Kalamazoo, MI 49008, USA

B. S. Hsiao
Department of Chemistry, Stony Brook University, Stony Brook, NY 11794, USA

Graphical abstract (Image was created with BioRender.com.)

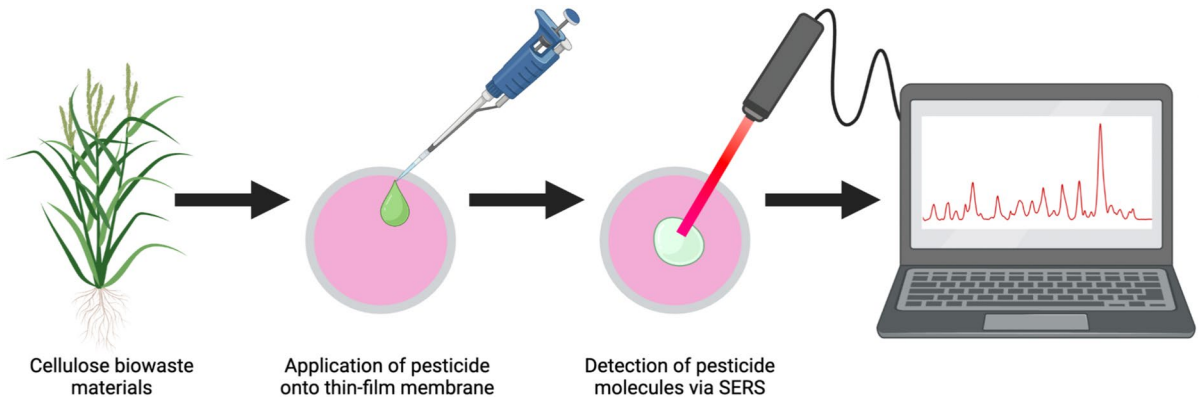

Keywords SERS · Raman · Pesticide · Nanocellulose

Introduction

As the human population continues to expand, it has become increasingly important for the agricultural sector to keep up with the growing demand for food crops. To protect agricultural products, pesticides are utilized to prevent crop damage from insects, rodents, fungi, and unwanted vegetation. Ever since pesticides were first introduced into agriculture, their usage has drastically increased (FAO 2000; Fernandez-Cornejo et al. 2014).

As a result, the prevalence of pesticides in the environment, specifically on unintended targets, has also escalated. For example, herbicides such as 2,4-dichlorophenoxyacetic acid and dicamba were shown to have lethal and sublethal effects on a non-target, beneficial insect (the lady beetle) (Freydier and Lundgren 2016), and the pesticide methoprene (used for mosquito control) has been shown to impact the hepatopancreas of the American lobster (Walker et al. 2010). If crops are contaminated unintentionally by pesticides, or if pesticides are applied in excess, there will be significant hazards to human health and food safety (Kim et al. 2017; Zikankuba et al. 2019). Pesticides entering ecological systems can have equally inimical effects. In 1952, the American Veterinary Medical Association attributed the parathion poisoning of geese to spray drift (Livingston 1952; Rattner 2009). In addition to animals on land, runoff entering marine systems can have exceedingly toxic effects on the biological systems; coral reef environments are particularly vulnerable to pesticides in the oceans (Markey et al. 2007). Pesticides can also enter freshwater systems and impact species diversity (Beketov et al. 2013). Terrestrial environments near agricultural lands are affected by contaminated runoff and show severe negative impacts on biodiversity (Jepson et al. 2014). Pesticides pose a significant risk to human health and can be taken into the body via direct exposure (such as inhalation) or through ingestion of contaminated food products or water (Kim et al. 2017; Mostafalou and Abdollahi 2013; Umapathi et al. 2022). Given their dangerous nature, it is imperative to be able to monitor pesticides within our environment.

Although pesticides have been detected in many aquatic and terrestrial environments, the detection of pesticides within agricultural spray droplets is underexplored. These droplets do not always land on the surface of the target agricultural products; at times, the aerosol spray may drift to unintended targets within the environment. In addition, the high surface-to-volume ratio of aerosol droplets allows them to be chemically transformed by solar radiation or other reactive trace gas molecules, potentially creating

more hazardous materials (Pöschl 2005). Given the widespread use of pesticide spraying globally, there is a need for the development of analytical methods to rapidly and sensitively detect pesticide aerosol droplets in the environment.

Some methods that have been employed for the detection of pesticide aerosol droplets include the use of water-sensitive paper, which was used in conjunction with image processing software to analyze spray deposition and coverage on apple trees (Witton et al. 2018). This method is only able to detect the deposition location of sprayed droplets, but not their chemical composition or concentration. Absorbent resin filters, such as those available in the Pesticide Action Network's commercially available Drift Catcher, have been used to monitor pesticide spray drift from farms onto school grounds. This drift catcher works by way of a vacuum pump which draws air in at a controlled rate and filters it through a tube with Supelco XAD-2 resin, trapping various chemicals. Following collection, the resins were analyzed at a lab via flame photometry and gas chromatography-mass spectrometry (Dalvie et al. 2014). These methods are limited by the complex and expensive instrumentation that is used for the analysis, and they must be completed within a lab using benchtop instruments by well-trained technicians. Flower-like origami paper-based electrochemical platforms have also been used to detect three pesticides through their interactions with three different enzymes within this device (Caratelli et al. 2022). While this device can be used for the detection of aerosols, it is designed for the selective detection of only three specific pesticides (paraoxon, 2,4-dichlorophenoxyacetic acid, and glyphosate) due to the lack of molecular fingerprinting ability in the electrochemical sensor.

Surface-enhanced Raman spectroscopy (SERS) is an advanced, rapid, and non-destructive method for chemical or biological analysis. The "enhancement" of the Raman spectroscopy is obtained by using specially designed nanostructures to increase the intensity of the obtained spectra. Noble metal nanoparticles (e.g., gold or silver nanoparticles) are commonly used to produce an electromagnetic and/or chemical enhancement of the Raman signals, up to magnitudes of 10^{10}–10^{11} (Anderson and Moskovits 2006; Le Ru et al. 2007; Blackie et al. 2009; Maher 2012; Pilot et al. 2019).

SERS requires little to no sample preparation and can be used on extremely small amounts of samples (down to single molecule detection) (Kneipp et al. 2001; Nie and Emory 1997; Pettinger 2010). Through this technique, unique fingerprint spectra can be produced for quantitative and qualitative analysis of a variety of analytes. However, there can be difficulties associated with the preparation of SERS substrates.

A particular challenge associated with the use of a liquid suspension of noble metal nanoparticles is the nonuniform drying of these particles on a particular surface. This can occur due to the "coffee ring effect", where capillary flow can cause particles to flow towards the edges of a droplet during the drying process (Huang et al. 2018). Substrates have been created in an attempt to mitigate this effect to create more uniform surfaces; one example involved immobilized silver cubic nanoparticles on titanium dioxide nanotubes, and another involved the creation of a hydrophobic surface from titanium dioxide coated aluminum plates with gold nanoparticles (Ambroziak et al. 2020; Breuch et al. 2022). However, these methods involved complex substrate preparation, and did not utilize sustainable materials. The use of nanocellulose may be able to remedy this. Nanocellulose-based materials have been used as a component of various types of membranes or filters, as they have useful absorptive and adsorptive properties, high flexibility, hydrophilic surfaces, high surface areas, and tunable shape and size (Voisin et al. 2017; Sharma et al. 2020). Nanocellulose exists as cellulose nanocrystals (CNCs), cellulose nanofibrils (CNFs; also called nano-fibrillated cellulose, NFCs), and bacterial nanocellulose (BNC) (Tahir et al. 2022). Previous studies utilized nanocellulose for SERS sensors, but they did so with nanocellulose derived from commercial or bacterial sources (Tian et al. 2016; Hu et al. 2021). A more sustainable and environmentally friendly option involves biowaste-derived nanocellulose materials; however, there is a lack of research regarding this material as a component of SERS substrates. With biowaste-derived nanocellulose, waste products from agricultural processes can be utilized instead of being destroyed or gathered in landfills. As far as we are aware, there are limited reports of using biowaste-derived nanocellulose to create SERS nanosubstrates for the detection of environmental contaminants.

The current study demonstrates the use of bio-waste-derived cellulose nanofibrils (CNFs) to create a SERS nanosubstrate. The objective of this study is to use the sustainable SERS nanosubstrate for the detection of pesticides in agricultural spray droplets. It was hypothesized that, in combination with gold nanoparticles (AuNPs), CNFs could be utilized to create a thin film that would provide a uniform Raman enhancement at various points on the surface and reduce the coffee ring effect on the substrate. To test this, three pesticides were selected to assess the robustness of the developed SERS nanosubstrate: ferbam (a fungicide), thiabendazole (a fungicide and parasiticide), and carbaryl (an insecticide). The thin-films were used in conjunction with a portable Raman spectrometer to detect various concentrations of each pesticide. Through this study, a cost-effective method is demonstrated to create a sensitive SERS nanosubstrate that can be used to detect pesticides in the spray solution and liquid droplets. This approach has a high potential to be applied on-site for rapid pesticide analysis on targeted and untargeted surfaces.

Experimental methods

Chemicals and materials

Cellulose nanofibrils (CNFs) was provided by Stony Brook University from the Hsiao Lab, which was prepared via a previously published method (Geng et al. 2017) using CNF derived from raw jute fibers. The concentration of the CNF suspension used was 0.95 wt%, which had a degree of oxidation of 1.45 mmol/g. Gold(III) chloride trihydrate ($HAuCl_4{\cdot}3H_2O$, CAS 16961-25-4) was purchased from Sigma Aldrich. Sodium citrate dihydrate ($C_6H_9Na_3O_9$, CAS 6132-04-03) was purchased from Fisher. Durapore® polyvinylidene fluoride (PVDF) membranes (0.1 um pore size, 47 mm diameter, hydrophilic) and 1-Naphthyl-N-methylcarbamate (carbaryl, $C_{12}H_{11}NO_2$, CAS 63-25-2) were obtained from Millipore Sigma. Iron(III) dimethyldithiocarbamate (ferbam, $C_9H_{18}FeN_3S_6$, CAS 14484-64-1) was procured from TCI America, and 2-(4-thiazolyl)benzimidazole (thiabendazole, $C_{10}H_7N_3S$, CAS 148-79-8) was purchased from Alfa Aesar. Acetone (C_3H_6O, CAS 67-64-1) was obtained from Fisher Chemical, and ethanol (C_2H_5OH, 200 proof, CAS 64-17-5) was from Pharmco. The water used in the experiments was ultrapure water (18.2 MΩ, Millipore) unless otherwise noted.

Synthesis of AuNPs

Spherical gold nanoparticles (AuNPs) were prepared based on a previously published method with minor changes (Bastús et al. 2011). Briefly, 75 mL sodium citrate dihydrate (2.2 mM) were heated in a round bottom flask fitted with a reflux condenser under constant stirring. Between 95–96 °C, 0.5 mL (25 mM) gold(III) chloride trihydrate was added promptly to the solution and allowed to stir for 10 min, forming 20 nm AuNP seeds. The reaction flask was cooled to a temperature between 87.5–90 °C, after which, every 2 min 0.5 mL 60 mM sodium citrate dihydrate and 0.5 mL 25 mM $HAuCl_4{\cdot}3H_2O$ were added for a total of 10 additions. Stirring continued for 30 min at 90 °C, and then the AuNPs were cooled to room temperature.

Characterization of materials

AuNPs were characterized by dynamic light scattering (DLS) on a Malvern Panalytical Lab Blue Zetasizer to measure the particle size and zeta potential. For each measurement, 5 replicates were completed and averaged. CNFs were imaged via transmission electron microscopy (TEM) at Stony Brook University (Fig. S1). The size and distribution of the AuNPs was further characterized through scanning electron microscopy (SEM) measurements using a Zeiss SUPRA 55-VP FEG-SEM and ImageJ for analysis.

Preparation of AuNPs/CNF SERS nanosubstrate

To create the SERS nanosubstrate, a AuNPs/CNF suspension was prepared by mixing 312.5 µL of an as-prepared AuNPs solution with 312.5 µL CNFs and 11.875 mL ultrapure water by vortexing at 1900 rpm for 1 min. After mixing AuNPs with CNFs, the AuNPs/CNF suspension was bright pink in appearance. Following this, the pH value of the AuNPs/CNF/water mixture was measured and adjusted (if needed) using either dilute H_2SO_4 or dilute NaOH, dropwise.

On a 47 mm Millipore vacuum filtration setup, a 47 mm PVDF membrane was centered on the setup

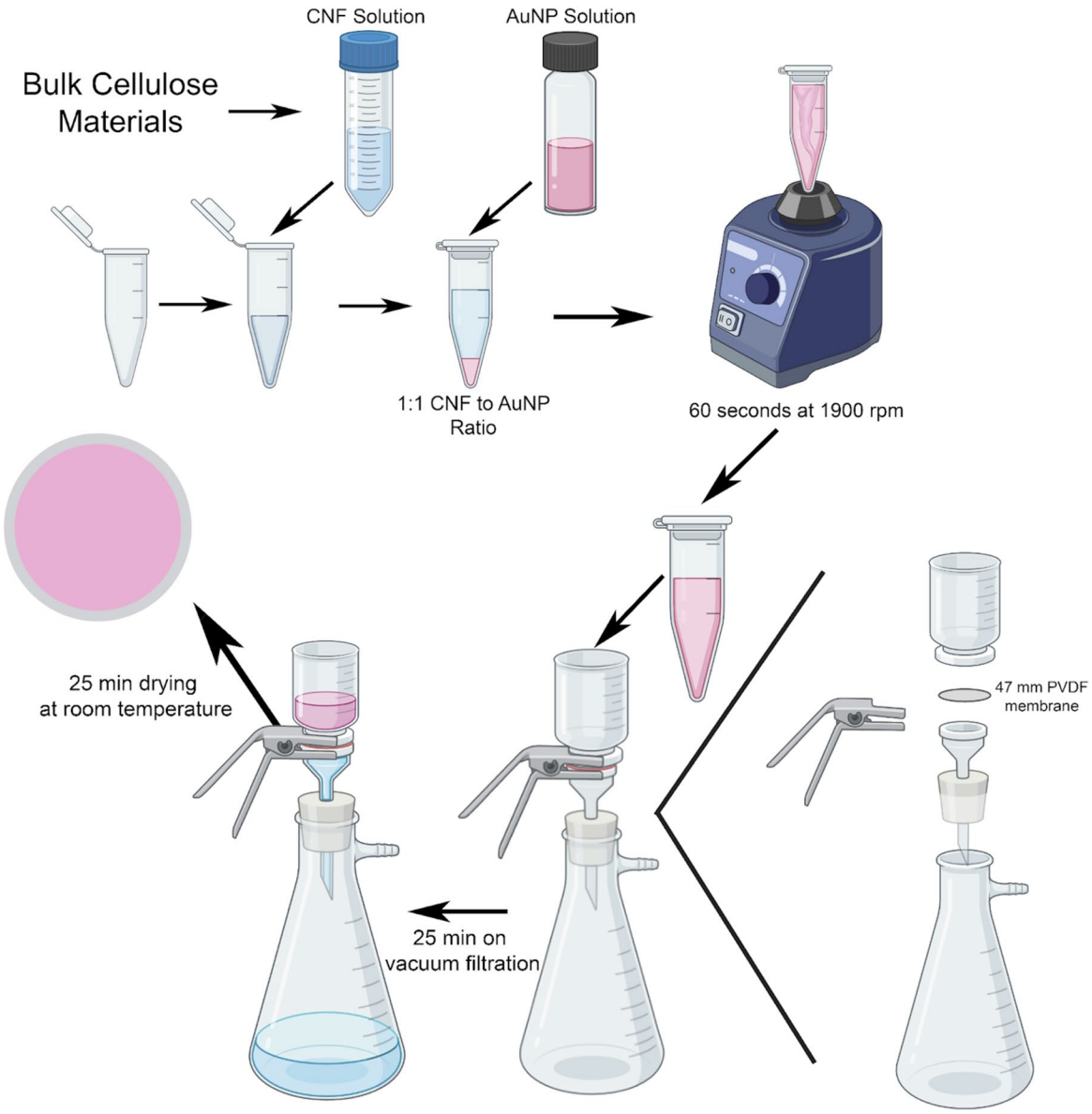

Fig. 1 Scheme showing the creation of AuNPs/CNF membrane via vacuum filtration at room temperature

and clamped between the filter flask and the 300 mL funnel. The vacuum filtration setup was the Millipore Classic Glass Filter Holder—Kit (47 mm, glass frit membrane support, 300 mL funnel, XX1014700). The 12.5 mL AuNPs/CNF suspension was poured over the PVDF membrane, while the vacuum was immediately applied. The membrane was dried for 25 min on the vacuum filtration setup, then removed from the setup and further dried for 25 min at room temperature. The edges of the membrane were held in place to prevent curling of the nanosubstrate. After drying on the PVDF, the thin-film was pink and shiny. The preparation of AuNPs/CNF SERS nanosubstrate is illustrated in Fig. 1. If not needed for immediate use, following preparation, the thin-film membranes were stored in a refrigerator in glass Petri dishes for future use.

Calibration curve and LOD determination for each pesticide on AuNPs/CNF thin-film nanosubstrate

A 1000 mg/L stock solution was prepared for each pesticide (using ethanol for carbaryl, and acetone for ferbam and thiabendazole). For the purposes of this study, mg/L concentrations are equivalent to ppm. From this stock, dilutions were made using ultrapure water. The prepared thin-film nanosubstrates were cut into several small pieces with scissors. A 2 µL droplet of the controls or pesticide solutions at different concentrations were applied to the center of the cut thin-film nanosubstrate piece positioned on a slide. The slides were allowed to dry at room temperature for 15 min prior to SERS analysis.

All Raman measurements were made on an EZRaman spectrometer (TSI ChemLogix, Enwave Optronics, Inc., EZRaman Reader V8.3.6), using a 785 nm laser with the following parameters: 5 s integration time, averaging of 2, boxcar of 1, 35 mW laser power (assessed using a laser power meter (ThorLabs PM100D)). For each sample, five measurements were taken at different locations within the sample droplet, unless otherwise noted. The average was used for the creation of applicable calibration curve plots based on the intensity of the Raman signals versus the concentration of each pesticide. The background SERS spectrum for the blank control was subtracted from all sample spectra.

The limit of detection (LOD) for each pesticide was determined through the use of the linear calibration curves and Eq. 1:

$$\mathrm{LOD} = \frac{3s}{m} \tag{1}$$

where s is the standard deviation of 5 replicates of blank control, and m is the slope of the linear calibration curve.

Method validation using spiked sprays and a commercial pesticide

To determine the applied concentration of pesticide from a spray applicator, a sprayer was used to spray 10 mg/L ferbam into a petri dish collector at a distance of 5 cm. A 2 µL sample of the sprayed ferbam was collected and applied to a piece of AuNPs/CNF thin-film nanosubstrate. In the same manner, a 2 µL volume of 10 mg/L ferbam from the original spray solution was applied to another piece of AuNPs/CNF nanosubstrate, and both experiments were repeated to produce three replicates for each sample. Samples were dried at room temperature for 15 min and then analyzed via SERS at five randomly selected positions within the droplet on each replicate. For commercial pesticide detection, Daconil concentrate was diluted to 25% original concentration with ultrapure water based on the manufacturer's instruction, and Daconil Ready-to-Use Spray was used as is. With these samples, 2 µL droplets were applied to a piece of AuNPs/CNF nanosubstrate, and the dried droplets were analyzed via SERS at five randomly selected points.

Results and discussion

Synthesis and characterization of AuNPs/CNF nanosubstrate

Figure 1 shows the process for the creation of the AuNPs/CNF thin-film nanosubstrate. After mixing AuNPs with CNFs, the AuNPs/CNF suspension was bright pink in appearance. Following deposition onto the 47 mm PVDF membranes, the dried sample became pink and shiny. The synthesized AuNPs were characterized using DLS and were found to have an average particle size of 50.85 ± 2.01 nm at 25 °C using the average of 5 scans in the side scatter mode. The zeta potential of the AuNPs was found to be -45.24 ± 3.25 mV using the average of 5 scans (Fig. S1). CNFs were imaged via transmission electron microscopy (TEM) at Stony Brook University (Fig. S2). CNF fibers had an average width of 7 nm, an average thickness of 1.5 nm, and an estimated length between 300–600 nm, as stated in a previous publication (Geng et al. 2017).

The AuNPs/CNF thin-film nanosubstrate was characterized using SEM (Fig. S3), which indicated that the average diameter of the AuNPs on the surface was 38.50 ± 4.69 nm (average diameter of 50 particles measured using ImageJ). The SEM images also showed the distribution of AuNPs across the surface of the thin-film nanosubstrate. It was noted that when greater concentrations of AuNP were utilized in the creation of the thin-film, the substrate was more prone to burning under the Raman laser, and the signal was thus decreased (Fig. S4).

The use of CNFs in the thin-film nanosubstrate visually reduces the "coffee ring effect" when compared with AuNPs drying on PVDF without CNFs (Fig. S5), creating a more uniform substrate. The coffee ring effect occurs when suspended nanoparticles travel towards the edge of the applied liquid during the drying process, creating a non-uniform distribution of the particles. A previous study utilized computational time-series image data to determine that CNF was useful in suppressing the coffee ring effect mechanically within dried colloidal droplets of microscale polystyrene particles (Ooi et al. 2017). They were able to determine that the addition of CNFs reduced the "rush hour" phenomena", where the speed of the particles traveling towards the edges of the droplet generally increase near the edges in the last stages of drying.

Optimization of pH for thin-film nanosubstrate preparation

SERS detection may be affected by the pH value because it controls the protonation and deprotonation of the functional groups on the SERS nanosubstrate surface, thus affecting the interactions between the analytes and the nanosubstrate, and the obtained spectra (Kazanci et al. 2009; Viviana et al. 2021). To obtain the highest Raman signal intensity, it is important to optimize the pH value. In the present study, the pH value of the AuNPs/CNF suspension was adjusted dropwise with either NaOH (0.1 M), or H_2SO_4 (0.1 M) to determine the pH value that could yield the maximum Raman intensity of each pesticide. The original pH of the unadjusted AuNPs/CNF suspension was 6.4. It was noted that at a pH value of 4, the thin-films became brittle and peeled away from the PVDF backing, and thus, this pH was not used for any further experiments beyond one test using ferbam (Fig. 2a). For each of the pesticides, a higher Raman intensity was obtained using the native pH of 6.4 than when using a pH of 8 (Fig. 2a–c), and so all subsequent nanosubstrates were created using unadjusted pH of 6.4 AuNPs/CNF suspension. The decreased signal intensity at a pH value of 8 is likely due to the deprotonated carboxyl group in CNF and increased negative charges, which caused the repulsion between CNFs and the target pesticides with either negative charges (ferbam) or lone electron pairs (carbaryl and thiabendazole).

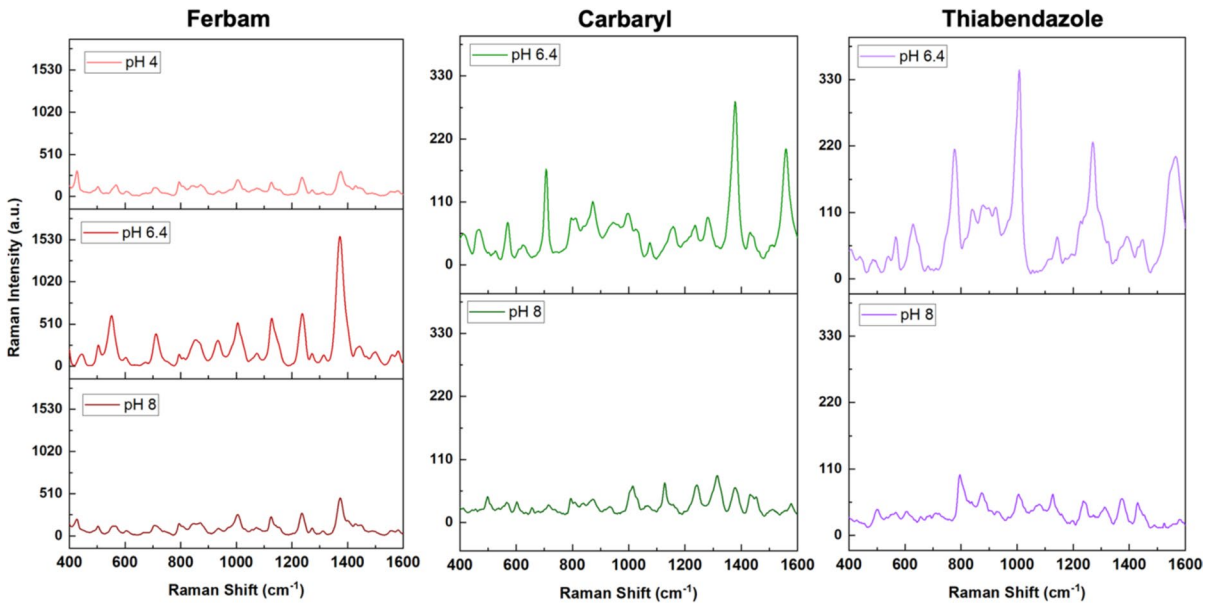

Fig. 2 SERS spectra for **a** ferbam, **b** carbaryl, and **c** thiabendazole as a function of pH during AuNPs/CNF preparation

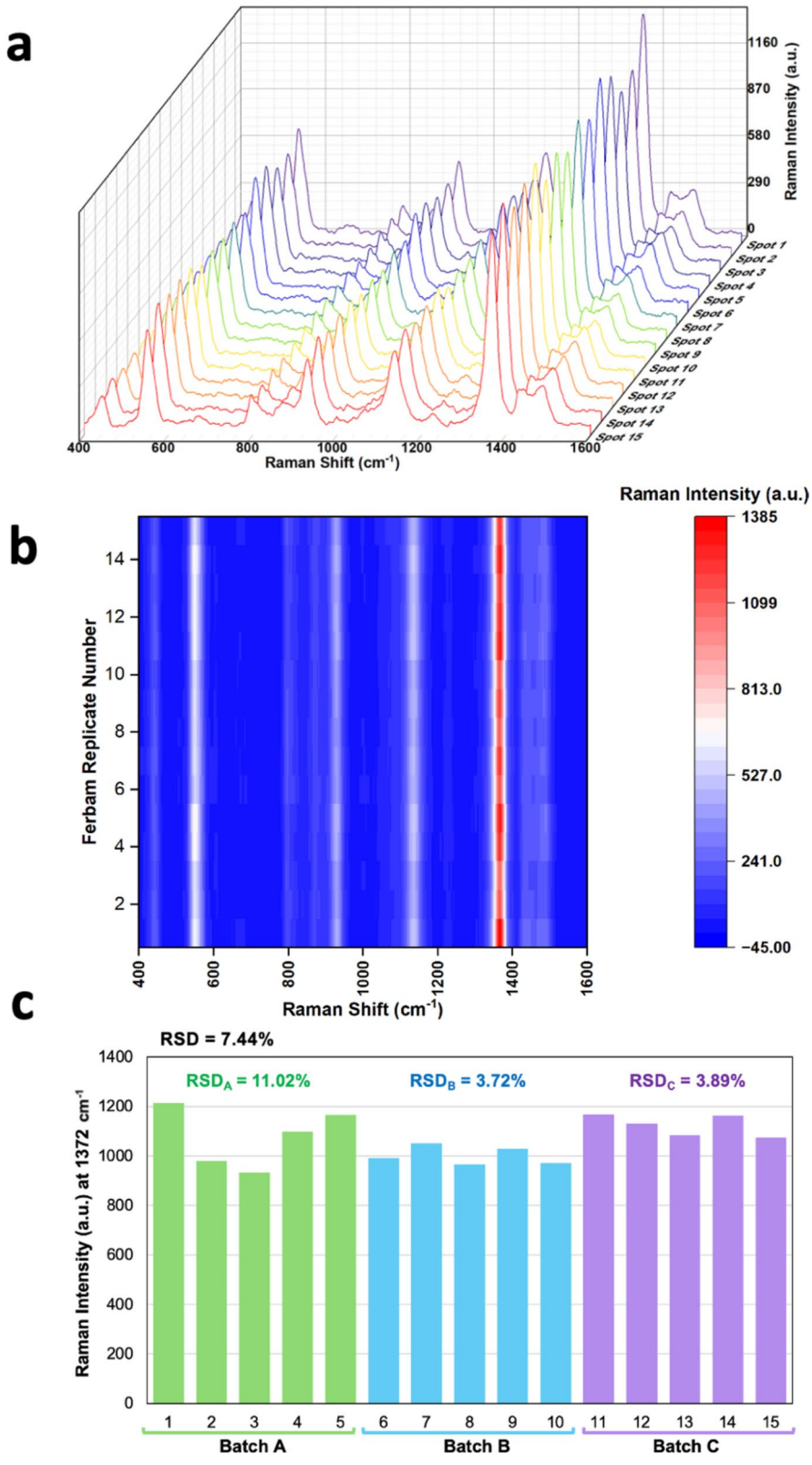

Fig. 3 Reproducibility of the SERS signals of a 1 µL droplet of 10 mg/L ferbam on AuNPs/CNF nanosubstrate. **a** 3D Waterfall plot for 15 replicate measurements, **b** heat map of Raman intensities for each replicate measurement, and **c** bar chart showing the intensity of the peak at 1372 cm^{-1} for each replicate, as well as the relative standard deviations

Reproducibility of the AuNPs/CNF nanosubstrate

The SERS nanosubstrate was evaluated for reproducibility across different AuNPs/CNF nanosubstrates and at different points on the surface of the same nanosubstrate. Figure 3a gives a visual representation of the SERS spectra for 15 replicate measurements of a 10 mg/L sample of ferbam on AuNPs/CNF nanosubstrate. Replicates 1–5 are five different points measured on a single AuNPs/CNF nanosubstrate (batch A), 6–10 are from another nanosubstrate (batch B), and 11–15 are from a third nanosubstrate (batch C). Figure 3b shows the 15 SERS spectra as a heat map, highlighting the uniform spectral pattern and signal intensity. Figure 3c shows the intensity of the peaks at 1372 cm^{-1} for each of the 15 replicate measurements, along with the relative standard deviations (RSD) for each batch (11.02% for batch A, 3.72% for batch B, and 3.89% for batch C); the overall RSD for the 15 replicate measurements is 8.22% for the peak position of 1372 cm^{-1}. The low RSD values indicate uniformity and reproducibility in the SERS signals for this material (Grys et al. 2021). Spectra for the background (CNFs or AuNPs/CNF) as well as Raman and SERS spectra for each of the pesticides are shown in Fig. S6. There is a greatly increased RSD for a substrate produced from only AuNPs (without any CNFs). This can be seen in Fig. S7, in which 15 replicate measurements of ferbam at 7 mg/L were taken on a substrate made only from AuNPs on PVDF; the RSD for these 15 replicates was 51.07%. Additional reproducibility data for carbaryl, ferbam, and thiabendazole at 20 mg/L on AuNPs/CNF substrates are shown in Fig. S8, S9, S10. A prior study utilizing a CNF/AuNP nanocomposite for SERS measurements of the Raman probe molecule, 4-aminothiophenol (4-ATP) collected SERS signals from 16 random positions within an area containing 5 ppm 4-ATP (Xiong et al. 2018). They achieved an RSD of 25.47% and considered the uniformity and reproducibility to be acceptable. Compared with that study, the current work has improved reproducibility and uniformity across the surface of the cellulose nanosubstrate.

Calibration curve and LOD determination for each pesticide on AuNPs/CNF nanosubstrate

To evaluate the potential of the approach to quantify pesticides, a range of concentrations for each pesticide were applied to the AuNPs/CNF thin-films.

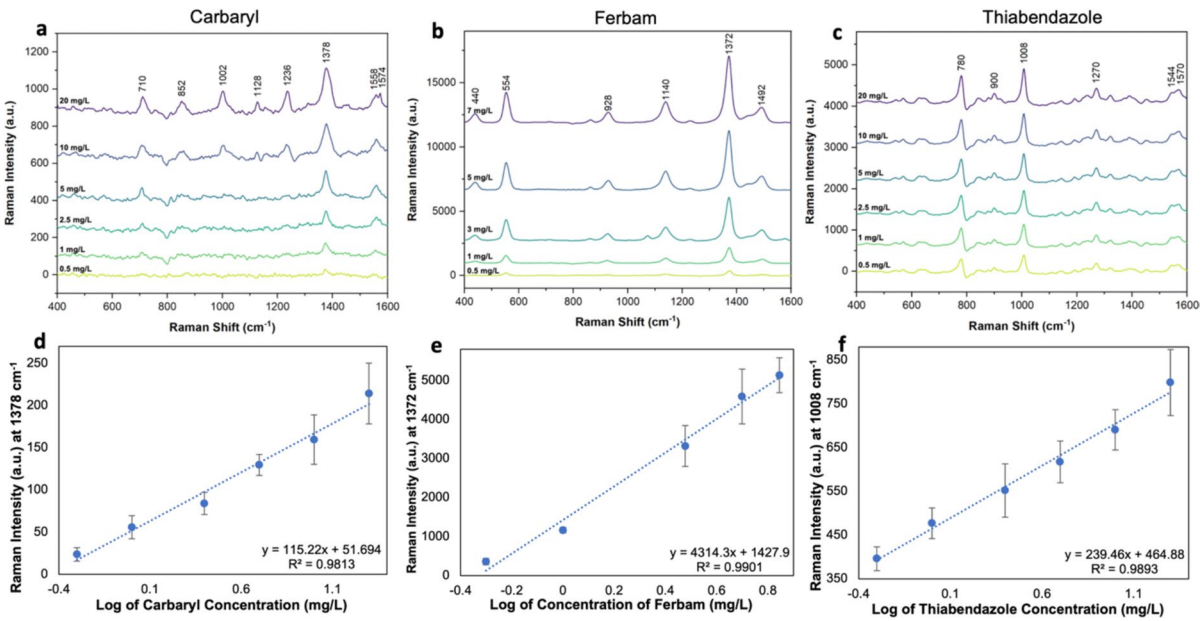

Fig. 4 SERS spectra from various concentrations of **a** carbaryl, **b** ferbam, and **c** thiabendazole; control signals have been subtracted from all spectra. Calibration curves are shown for **d** carbaryl, **e** ferbam, and **f** thiabendazole, where the x-axis is the log of the concentration

Each pesticide concentration with 5 replicates was measured by SERS. The average spectrum for each concentration is shown in Fig. 4 for carbaryl (Fig. 4a), ferbam (Fig. 4b), and thiabendazole (Fig. 4c), respectively, along with associated calibration curves (Fig. 4d–f). Each of the 5 replicate measurements utilized to provide the average SERS spectra for each concentration of each of the 3 pesticides is presented in Fig. S8, S9, and S10. Logarithmic curves were fit to a larger concentration range for each pesticide, and these are shown in Fig. S11. The logarithmic curves suggest that the pesticide may be saturating the thin-film nanosubstrate at higher concentrations, blocking the enhancement from the AuNPs. These spectra demonstrate that a range of concentrations of each pesticide can be identified and quantitatively analyzed using the developed thin-film nanosubstrate in conjunction with SERS. From these calibration curves, the LOD values for each pesticide were determined to be 1.34, 1.01, and 1.41 mg/L for carbaryl, ferbam, and thiabendazole, respectively. According to the user guide on product labels of the corresponding commercial pesticide products Ferbam Granuflo® (Taminco), Loveland's Carbaryl 4L (Loveland Products Inc.), Thiabendazole 4L ST Fungicide by Agri Star (Agri Star), and Thiabendazole 4.1 FL AG (Albaugh 2015), the LODs achieved in this study are well below the concentrations recommended by manufacturers for application in agricultural settings. Carbaryl is recommended to be applied at approximately 239,653 mg/L (Loveland Products Inc.), ferbam is recommended to be applied between 1047–8195 mg/L (Taminco), and thiabendazole is recommended to be applied between 1534–3500 mg/L (Agri Star; Albaugh 2015).

Differentiation of pesticides on AuNPs/CNF nanosubstrate

To determine if each of the three pesticides could be differentiated from one another, each pesticide solution was applied to pieces of the developed AuNPs/CNF nanosubstrate. The Raman peaks for each pesticide were labeled (using OriginLab Pro software),

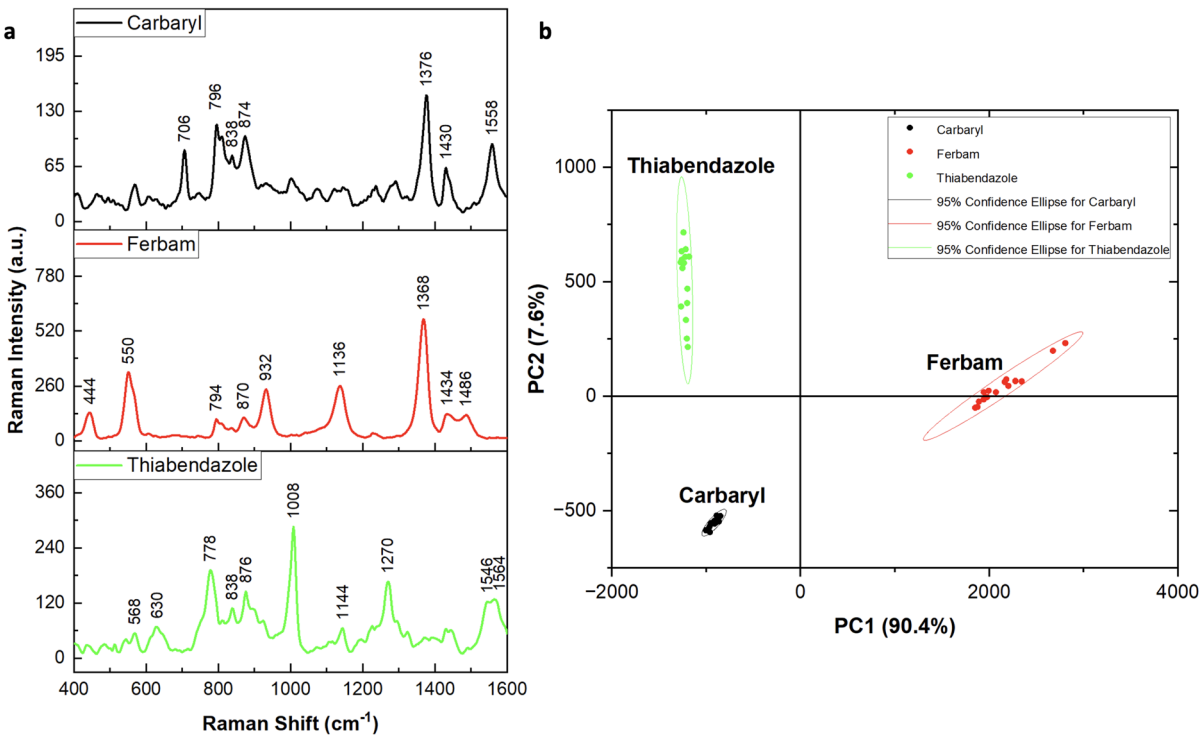

Fig. 5 **a** SERS spectra from 20 mg/L carbaryl, ferbam, and thiabendazole droplets on AuNPs/CNF nanosubstrate; **b** PCA analysis (from OriginLab Pro) showing 95% confidence ellipses for 15 spectra obtained for each pesticide

including prominent peaks at 796, 1376, 1430 and 1558 cm^{-1} for carbaryl, 444, 550, 1136, and 1368 cm^{-1} for ferbam, and 778, 876, 1008, 1270, and 1564 cm^{-1} for thiabendazole (Fig. 5a). These peak locations are in good agreement with previously published values. For carbaryl, our peak around 1558 cm^{-1} matches with the 1568 cm^{-1} peak, and our 1430 cm^{-1} peak matches with a peak at 1440 cm^{-1} (Nowicka et al. 2019). For ferbam, our peaks at 444, 550, and 1368 cm^{-1} agree with 441, 563, and 1382 cm^{-1}, respectively (Hussain et al. 2021). Looking at thiabendazole, our peaks at 778, 876, 1008, 1270, and 1564 cm^{-1} match with published values of 779, 879, 1278, and 1578 cm^{-1}, respectively (Hussain et al. 2021).

A principal component analysis (PCA) was performed using OriginLab Pro software, where 3 replicates were scanned at 5 random points each to

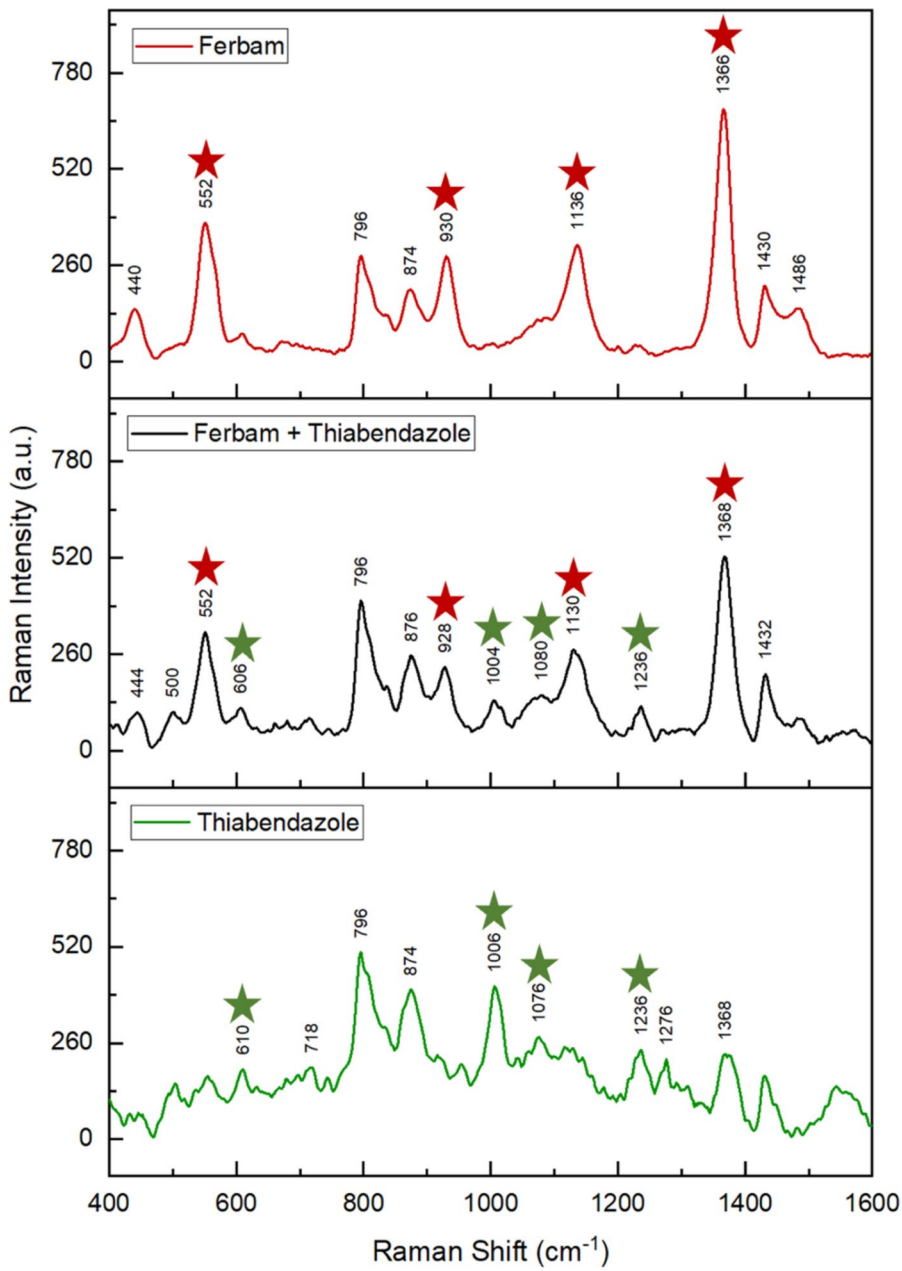

Fig. 6 SERS spectra of 10 mg/L ferbam (top), a mixture of 10 mg/L ferbam with 20 mg/L thiabendazole (middle), and 20 mg/L thiabendazole (bottom), with characteristic peaks labeled. Peaks within the mixture are labeled for those that match with ferbam (red stars), and for those that match with thiabendazole (green stars)

accumulate 15 spectra for each pesticide. The resulting data are shown (Fig. 5b) with 95% confidence ellipses for each set of spectra. Each pesticide's data points are mainly clustered within the 95% confidence ellipses, indicating that the pesticides can be differentiated based on the SERS spectra using our approach.

In agriculture, oftentimes multiple pesticides are applied to the same target crop for different pests. It is important to test the feasibility of the method to detect and identify each pesticide. Other methods (HPLC, GC, HPLC–MS, or GC–MS) can be used to differentiate compounds, but require more costly instruments, more extensive sample preparation, or are more expensive to run (Gong et al. 2019; Xu et al. 2023). To determine whether pesticides could be differentiated within a mixture using the AuNPs/CNF thin-film, pesticide solutions were mixed in a 1:1 volume ratio and applied to the AuNPs/CNF and analyzed via SERS. Compared with the reference spectrum from each pesticide (Fig. 6), peaks that are unique to ferbam (552, 930, 1136, and 1366 cm^{-1}) and thiabendazole (610, 1006, 1076, and 1236 cm^{-1}) both appear in the spectrum from the mixture of the two pesticides, suggesting that the developed thin-films are able to be utilized for the selective detection of a pesticide in the mixture.

Determination of pesticides in spiked sprays on AuNPs/CNF nanosubstrate

When pesticides are applied, not all the sprayed pesticide can reach the target crop. A significant portion of pesticides may be released into areas surrounding the intended crops (Duke 2017). Some of this movement is caused by spray drift, where droplets travel away from the area where they were applied due to air movements; this can cause a significant threat to human health and the environment (Bedos et al. 2013; Perine et al. 2021; Prechsl et al. 2022). To test whether our method can be used to detect sprayed pesticides reliably, a sample of 10 mg/L ferbam was tested both using the original spray solution and the spray droplets collected after spraying. The results are displayed using a box-and-whisker plot (Fig. 7). A, B, and C indicate the three replicates for either condition; five data points were collected on each sample via SERS. Exclusive median was used to generate the plot on Excel. The comparison shows that there is

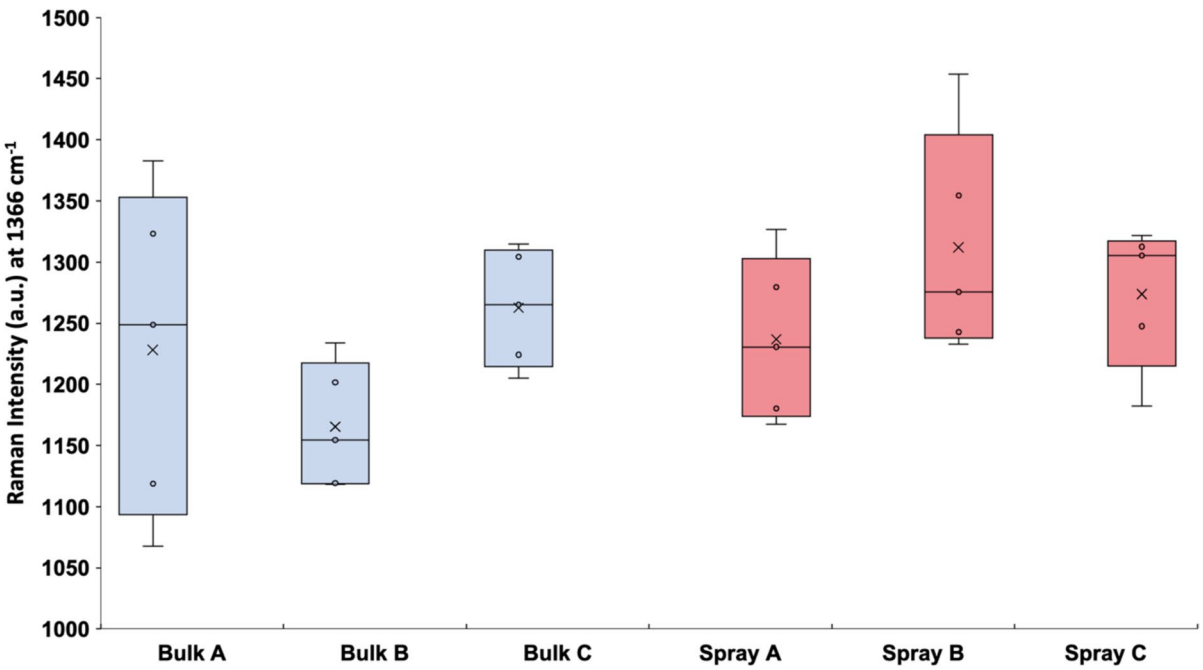

Fig. 7 Box-and-whisker plot of the SERS intensity (a.u.) of 10 mg/L ferbam at 1366 cm^{-1} from either the bulk solution (original spray solution), or from droplets collected after being sprayed

not a major difference in the SERS intensity between the original ferbam solution versus the spray droplets collected from the sprayed pesticide, indicating the reliability of our approach to detect pesticides in spray droplets. This will help growers determine the location and distribution of the sprayed pesticides and potential drifts, facilitating the evaluation of the application effectiveness.

Detection of commercially-available pesticides on AuNPs/CNF nanosubstrate

To determine whether the thin-film nanosubstrate could be used to detect a pesticide within a more complex matrix, a commercially available fungicide, Daconil, was used in concentrated form (29.6% chlorothalonil, active ingredient) and in Ready-To-Use (RTU) Spray form (0.087% chlorothalonil). This product is readily available to consumers at home improvement and garden stores. Chlorothalonil is a broad spectrum fungicide which is toxic to aquatic organisms and its metabolites are persistent and highly mobile in the environment (Lv et al. 2022). This pesticide was selected for use as it was readily available from the market, and also because commercial formulations of carbaryl, ferbam, and thiabendazole were not able to be purchased for research use due to the strict regulations. Fig. S12 shows the average of 5 Raman spectra for droplets of a 25% dilution of Daconil Concentrate, as well as droplets of RTU Spray on AuNPs/CNF thin-film nanosubstrate. Prominent peaks are visible at 1264 cm^{-1}, between 1490–1526 cm^{-1}, between 1530–1550 cm^{-1}, and between 2228–2240 cm^{-1}, which are in good agreement with previously published reference Raman spectra for chlorothalonil (Yu et al. 2021; Wu et al. 2022). Through this, it is clear that the thin-film nanosubstrate enhances the signals of the target pesticide without interference by other ingredients in the commercial formula. This demonstrates the high potential of using the method developed here to detect real-world pesticide formulas in agricultural settings.

Conclusions

This study is among the first to utilize biowaste-derived nanocellulose to create SERS nanosubstrate for pesticide detection in spray droplets. Specifically, nanocellulose was utilized to produce a uniform distribution of AuNPs across the thin-film surface, enabling reliable and reproducible SERS measurements. The demonstrated AuNPs/CNF nanosubstrate can provide sensitive detection of pesticides down to LODs of 1.34, 1.01, and 1.41 mg/L for carbaryl, ferbam, and thiabendazole, respectively. Additionally, this nanosubstrate can be used to differentiate the pesticides from one another based on the identification of their characteristic SERS peaks. It was found that there is not a major difference in SERS signal intensity between the original pesticide solution and the droplets collected from the pesticide spray. The thin-film nanosubstrate was also able to enhance the signals for the active ingredient, chlorothalonil, within a commercial pesticide, demonstrating promising applications for commercial pesticide products. Since the AuNPs/CNF thin-film nanosubstrate is coupled with a portable Raman spectrometer, this method has the potential for pesticide detection in the field. This approach can be useful to protect environmental safety and agricultural sustainability by taking advantage of sustainable biowaste-derived materials, simple nanosubstrate and sample preparation, as well as rapid, reproducible and sensitive analysis of pesticides.

Acknowledgements We acknowledge the financial support from the SUNY Research Foundation startup fund [RF Award 61476]. Also, this work was supported by the SUNY System Administration under the SUNY Research Seed Grant Award [Award# 95216], and the Binghamton Bridges to the Baccalaureate Summer Research Internship Program. BSH thanks the partial financial support of this work by a National Science Foundation Grant (NSF-DMR-2216585).

Author contributions HG and LRT contributed to the study conception and design. Material preparation was prepared at Stony Brook University by BSH and PS; further material preparation and data collection and analysis were performed at Binghamton University by LRT, JWK, MJ, and AL under the supervision of HG. The first draft of the manuscript was prepared by LRT, and all authors revised further drafts. All authors read and approved the final manuscript.

Funding This work was supported by from the SUNY Research Foundation startup fund [RF Award 61476]. Also, this work was supported by the SUNY System Administration under the SUNY Research Seed Grant Award [Award# 95216], and the Binghamton Bridges to the Baccalaureate Summer Research Internship Program. BSH thanks the partial financial support of this work by a National Science Foundation Grant (NSF-DMR-2216585).

Data availability No datasets were generated or analysed during the current study.

Declarations

Competing interests The authors declare no competing interests.

Ethical approval Not applicable.

References

Agri Star A Thiabendazole 4L ST Fungicide

Albaugh LLC (2015) THIABENDAZOLE 4.1 FL AG Fungicide

Ambroziak R, Krajczewski J, Pisarek M, Kudelski A (2020) Immobilization of cubic silver plasmonic nanoparticles on TiO2 nanotubes, reducing the coffee ring effect in surface-enhanced Raman spectroscopy applications. ACS Omega 5:13963–13972. https://doi.org/10.1021/acsomega.0c01356

Anderson DJ, Moskovits M (2006) A SERS-active system based on silver nanoparticles tethered to a deposited silver film. J Phys Chem B 110:13722–13727. https://doi.org/10.1021/jp055243y

Bastús NG, Comenge J, Puntes V (2011) Kinetically controlled seeded growth synthesis of citrate-stabilized gold nanoparticles of up to 200 nm: size focusing versus Ostwald ripening. Langmuir 27:11098–11105. https://doi.org/10.1021/la201938u

Bedos C, Loubet B, Barriuso E (2013) Gaseous deposition contributes to the contamination of surface waters by pesticides close to treated fields. A process-based model study. Environ Sci Technol 47:14250–14257. https://doi.org/10.1021/es402592n

Beketov MA, Kefford BJ, Schäfer RB, Liess M (2013) Pesticides reduce regional biodiversity of stream invertebrates. Proc Natl Acad Sci U S A 110:11039–11043. https://doi.org/10.1073/pnas.1305618110

Blackie EJ, Le Ru EC, Etchegoin PG (2009) Single-molecule surface-enhanced Raman spectroscopy of nonresonant molecules. J Am Chem Soc 131:14466–14472. https://doi.org/10.1021/ja905319w

Breuch R, Klein D, Moers C et al (2022) Development of gold nanoparticle-based SERS substrates on TiO2-coating to reduce the coffee ring effect. Nanomaterials (Basel) 12:860. https://doi.org/10.3390/nano12050860

Caratelli V, Fegatelli G, Moscone D, Arduini F (2022) A paper-based electrochemical device for the detection of pesticides in aerosol phase inspired by nature: a flower-like origami biosensor for precision agriculture. Biosens Bioelectron 205:114119. https://doi.org/10.1016/j.bios.2022.114119

Dalvie MA, Sosan MB, Africa A et al (2014) Environmental monitoring of pesticide residues from farms at a neighbouring primary and pre-school in the Western Cape in South Africa. Sci Total Environ 466–467:1078–1084. https://doi.org/10.1016/j.scitotenv.2013.07.099

Duke SO (2017) Pesticide dose—a parameter with many implications. In: Pesticide dose: effects on the environment and target and non-target organisms. American Chemical Society, Washington, pp 1–13

FAO (2000) Faostat: FAO statistical databases. Food & Agriculture Organization of the United Nations (FAO), Rome

Fernandez-Cornejo J, Nehring RF, Craig O, Wechsler S, et al (2014) Pesticide use in U.S. agriculture: 21 selected crops, 1960–2008

Freydier L, Lundgren JG (2016) Unintended effects of the herbicides 2,4-D and dicamba on lady beetles. Ecotoxicology 25:1270–1277. https://doi.org/10.1007/s10646-016-1680-4

Geng L, Peng X, Zhan C et al (2017) Structure characterization of cellulose nanofiber hydrogel as functions of concentration and ionic strength. Cellulose 24:5417–5429. https://doi.org/10.1007/s10570-017-1496-2

Gong X, Tang M, Gong Z et al (2019) Screening pesticide residues on fruit peels using portable Raman spectrometer combined with adhesive tape sampling. Food Chem 295:254–258. https://doi.org/10.1016/j.foodchem.2019.05.127

Grys D, Chikkaraddy R, Kamp M et al (2021) Eliminating irreproducibility in SERS substrates. J Raman Spectrosc 52:412–419. https://doi.org/10.1002/jrs.6008

Hu B, Pu H, Sun D-W (2021) Multifunctional cellulose based substrates for SERS smart sensing: principles, applications and emerging trends for food safety detection. Trends Food Sci Technol 110:304–320. https://doi.org/10.1016/j.tifs.2021.02.005

Huang Z, Nagpal A, Siddhanta S, Barman I (2018) Leveraging coffee-ring effect on plasmonic paper substrate for sensitive analyte detection using Raman spectroscopy. J Raman Spectrosc 49:1552–1558. https://doi.org/10.1002/jrs.5415

Hussain A, Pu H, Hu B, Sun D-W (2021) Au@Ag-TGANPs based SERS for facile screening of thiabendazole and ferbam in liquid milk. Spectrochim Acta A Mol Biomol Spectrosc 245:118908. https://doi.org/10.1016/j.saa.2020.118908

Jepson PC, Guzy M, Blaustein K et al (2014) Measuring pesticide ecological and health risks in West African agriculture to establish an enabling environment for sustainable intensification. Philos Trans R Soc Lond B Biol Sci 369:20130491. https://doi.org/10.1098/rstb.2013.0491

Kazanci M, Schulte JP, Douglas C et al (2009) Tuning the surface-enhanced Raman scattering effect to different molecular groups by switching the silver colloid solution pH. Appl Spectrosc 63:214–223. https://doi.org/10.1366/000370209787391987

Kim K-H, Kabir E, Jahan SA (2017) Exposure to pesticides and the associated human health effects. Sci Total Environ 575:525–535. https://doi.org/10.1016/j.scitotenv.2016.09.009

Kneipp K, Kneipp H, Itzkan I, et al (2001) Single molecule detection using near infrared surface-enhanced Raman scattering. In: Single molecule spectroscopy. Springer, Berlin, pp 144–160

Le Ru EC, Blackie E, Meyer M, Etchegoin PG (2007) Surface enhanced Raman scattering enhancement factors: a comprehensive study. J Phys Chem C 111:13794–13803. https://doi.org/10.1021/jp0687908

Livingston ML (1952) Parathion poisoning in geese. J Am Vet Med Assoc 120:27

Loveland Products Inc. CARBARYL 4L
Lv P, Wang Y, Zheng X et al (2022) Selective, stepwise photodegradation of chlorothalonil, dichlobenil and dichloro- and trichloro-isophthalonitriles enhanced by cyanidin in water. Sci Total Environ 805:150157. https://doi.org/10.1016/j.scitotenv.2021.150157
Maher RC (2012) SERS hot spots. In: Kumar CSSR (ed) Raman spectroscopy for nanomaterials characterization. Springer, Berlin, pp 215–260
Markey KL, Baird AH, Humphrey C, Negri AP (2007) Insecticides and a fungicide affect multiple coral life stages. Mar Ecol Prog Ser 330:127–137. https://doi.org/10.3354/meps330127
Mostafalou S, Abdollahi M (2013) Pesticides and human chronic diseases: evidences, mechanisms, and perspectives. Toxicol Appl Pharmacol 268:157–177. https://doi.org/10.1016/j.taap.2013.01.025
Nie S, Emory SR (1997) Probing single molecules and single nanoparticles by surface-enhanced Raman scattering. Science (1979) 275:1102–1106. https://doi.org/10.1126/science.275.5303.1102
Nowicka AB, Czaplicka M, Kowalska AA et al (2019) Flexible PET/ITO/Ag SERS platform for label-free detection of pesticides. Biosensors (Basel) 9:111. https://doi.org/10.3390/bios9030111
Ooi Y, Hanasaki I, Mizumura D, Matsuda Y (2017) Suppressing the coffee-ring effect of colloidal droplets by dispersed cellulose nanofibers. Sci Technol Adv Mater 18:316–324. https://doi.org/10.1080/14686996.2017.1314776
Perine J, Anderson JC, Kruger GR et al (2021) Effect of nozzle selection on deposition of thiamethoxam in Actara® spray drift and implications for off-field risk assessment. Sci Total Environ 772:144808. https://doi.org/10.1016/j.scitotenv.2020.144808
Pettinger B (2010) Single-molecule surface- and tip-enhanced Raman spectroscopy. Mol Phys 108:2039–2059. https://doi.org/10.1080/00268976.2010.506891
Pilot R, Signorini R, Christian D, Orian L et al (2019) A review on surface-enhanced Raman scattering. Biosensors (Basel) 9:57. https://doi.org/10.3390/bios9020057
Pöschl U (2005) Atmospheric aerosols: composition, transformation, climate and health effects. Angew Chem Int Ed Engl 44:7520–7540. https://doi.org/10.1002/anie.200501122
Prechsl UE, Bonadio M, Wegher L, Oberhuber M (2022) Long-term monitoring of pesticide residues on public sites: a regional approach to survey and reduce spray drift. Front Environ Sci Eng China 10:1062333. https://doi.org/10.3389/fenvs.2022.1062333
Rattner BA (2009) History of wildlife toxicology. Ecotoxicology 18:773–783. https://doi.org/10.1007/s10646-009-0354-x
Sharma PR, Sharma SK, Lindström T, Hsiao BS (2020) Nanocellulose-enabled membranes for water purification: perspectives. Adv Sustain Syst 4:1900114. https://doi.org/10.1002/adsu.201900114
Tahir D, Karim MRA, Hu H et al (2022) Sources, chemical functionalization, and commercial applications of nanocellulose and nanocellulose-based composites: a review. Polymers (Basel) 14:4468. https://doi.org/10.3390/polym14214468
Taminco Ferbam Granuflo® Fungicide. 8
Tian L, Jiang Q, Liu K-K et al (2016) Bacterial nanocellulose-based flexible surface enhanced Raman scattering substrate. Adv Mater Interfaces 3:1600214. https://doi.org/10.1002/admi.201600214
Umapathi R, Park B, Sonwal S et al (2022) Advances in optical-sensing strategies for the on-site detection of pesticides in agricultural foods. Trends Food Sci Technol 119:69–89. https://doi.org/10.1016/j.tifs.2021.11.018
Viviana MN, Renda V, Trusso S, Ponterio RC (2021) Role of pH on nanostructured SERS active substrates for detection of organic dyes. Molecules. https://doi.org/10.3390/molecules26082360
Voisin H, Bergström L, Liu P, Mathew AP (2017) Nanocellulose-based materials for water purification. Nanomaterials (Basel) 7:57. https://doi.org/10.3390/nano7030057
Walker AN, Golden R, Horst MN (2010) Morphologic effects of in vivo acute exposure to the pesticide methoprene on the hepatopancreas of a non-target organism, Homarus americanus. Ecotoxicol Environ Saf 73:1867–1874. https://doi.org/10.1016/j.ecoenv.2010.08.013
Witton JT, Pickering MD, Alvarez T et al (2018) Quantifying pesticide deposits and spray patterns at micro-scales on apple (Malus domesticus) leaves with a view to arthropod exposure. Pest Manag Sci 74:2884–2893. https://doi.org/10.1002/ps.5136
Wu G, Li W, Du W et al (2022) In-situ monitoring of nitrile-bearing pesticide residues by background-free surface-enhanced Raman spectroscopy. Chin Chem Lett 33:519–522. https://doi.org/10.1016/j.cclet.2021.06.051
Xiong Z, Lin M, Lin H, Huang M (2018) Facile synthesis of cellulose nanofiber nanocomposite as a SERS substrate for detection of thiram in juice. Carbohydr Polym 189:79–86. https://doi.org/10.1016/j.carbpol.2018.02.014
Xu R, Dai S, Dou M et al (2023) Simultaneous, label-free and high-throughput SERS detection of multiple pesticides on Ag@Three-Dimensional silica photonic microsphere array. J Agric Food Chem 71:3050–3059. https://doi.org/10.1021/acs.jafc.2c07846
Yu H, Xu L, Yang F et al (2021) Rapid surface-enhanced Raman spectroscopy detection of chlorothalonil in standard solution and orange peels with pretreatment of ultraviolet irradiation. Bull Environ Contam Toxicol 107:221–227. https://doi.org/10.1007/s00128-021-03258-9
Zikankuba VL, Mwanyika G, Ntwenya JE, James A (2019) Pesticide regulations and their malpractice implications on food and environment safety. Cogent Food Agric 5:1601544. https://doi.org/10.1080/23311932.2019.1601544